

## Small Molecule Binding to Proteins: Affinity and Binding/Unbinding Dynamics from Atomistic Simulations

Danzhi Huang\* and Amedeo Caflisch\*[a]

Several experimental<sup>[1,2]</sup> and computational<sup>[3]</sup> approaches to fragment-based drug design have been developed during the past 15 years. The experimental methods are still limited in their temporal and spatial resolution, while the computational techniques suffer from insufficient accuracy, particularly in the evaluation of binding affinity. Recently, molecular dynamics (MD) simulations have been used for flexible docking, i.e., to determine the binding modes of low-molecular-weight fragments to proteins,<sup>[4,5]</sup> however, binding affinity and kinetics were not investigated. Simulations of biased unbinding of small molecules from antibodies,<sup>[6]</sup> enzymes,<sup>[7,8]</sup> and receptors<sup>[9,10]</sup> have been reported but the external pulling force alters the free-energy landscape significantly.

In a previous work, we studied the free-energy surface and pathways of unbinding of six small ligands (4–11 nonhydrogen atoms) from the active site of FKBP—the FK506 binding protein that is also a peptidyl-prolyl *cis-trans* isomerase—by explicit solvent MD simulations started from the X-ray structure of the complex.<sup>[11]</sup> Here, without employing any information on the binding mode, we determine the locations and residence times of dimethylsulfoxide (DMSO) on the FKBP surface by means of multiple MD runs using high concentrations of DMSO in the simulation box.

Most of the following analysis is based on ten independent 70 ns MD runs at 310 K with a DMSO concentration of 0.44 M, i.e., 50 DMSO molecules and one FKBP molecule in a 57 Å-cubic box. Essentially identical results (binding modes, affinities, kinetics) were obtained in MD simulations with DMSO concentrations larger or smaller by a factor of two, as expected because of the very high solubility of DMSO in water.<sup>[12]</sup> The simulations were started from ran-

domly dispersed DMSO molecules in the bulk water. The MD sampling of 0.7 μs required about two days on 80 processors of type Xeon 5500 2.8 GHz (see Supporting Information for details of simulation protocols and analysis methods). The programs CHARMM<sup>[13]</sup> and WORDOM<sup>[14]</sup> were used for the analysis of the MD trajectories. The latter program was employed to calculate the frequency of each DMSO/FKBP contact, which is defined as an interatomic distance smaller than 6 Å. [Note that this analysis is robust with respect to the choice of distance threshold (see Supporting Information).]

The mapping of the contact frequencies on the surface of FKBP (Figure 1) indicates that the main location is at the active

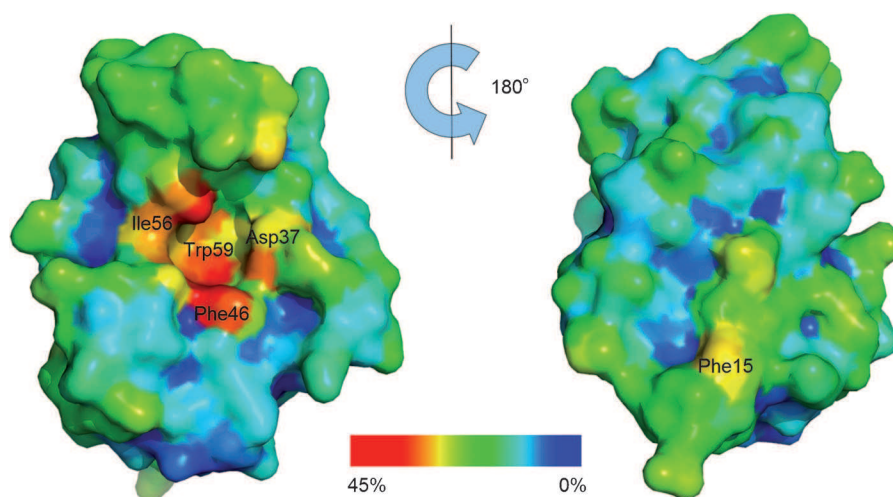


**Figure 1.** Map of DMSO/FKBP contact frequencies. The surface of FKBP is colored according to the percentage of MD snapshots in which the center of mass of any of the 50 DMSO molecules is within 6 Å of any nonhydrogen atom of FKBP. The active site (left) with Trp59 at its bottom is the main binding site of DMSO, in agreement with experimental data,<sup>[12,15]</sup> while the second most frequent interaction site is at residue Phe15, the side chain of which is on the opposite region of the FKBP surface with respect to the active site (right).

site, and another minor location is close to Phe15. In the main binding mode, DMSO accepts a hydrogen bond from the backbone amide NH of Ile56 and the DMSO methyl groups are in van der Waals contact with the side chains of Tyr26, Phe46, Val55, Trp59, and Phe99, in agreement with the X-ray structure (Figure 2a) and NMR spectroscopy data.<sup>[12]</sup> Furthermore, the distance distribution of the second closest DMSO shows that there is only one DMSO molecule in the active site (Supporting Information). In the minor location, the DMSO methyl groups interact with the phenyl ring of Phe15, while the sulfinyl oxygen atom points towards the solvent.

The large number of binding and unbinding events to and from the active site (more than 100 in each direction) allows the on- and off-rates to be extracted from the MD runs. The

[a] D. Huang, A. Caflisch

Department of Biochemistry, University of Zürich  
Winterthurerstrasse 190, 8057 Zürich (Switzerland)  
Fax: (+41) 44-635 68 62  
E-mail: dhuang@bioc.uzh.ch  
caflisch@bioc.uzh.ch

Supporting information for this article is available on the WWW under <http://dx.doi.org/10.1002/cmdc.201100237>.

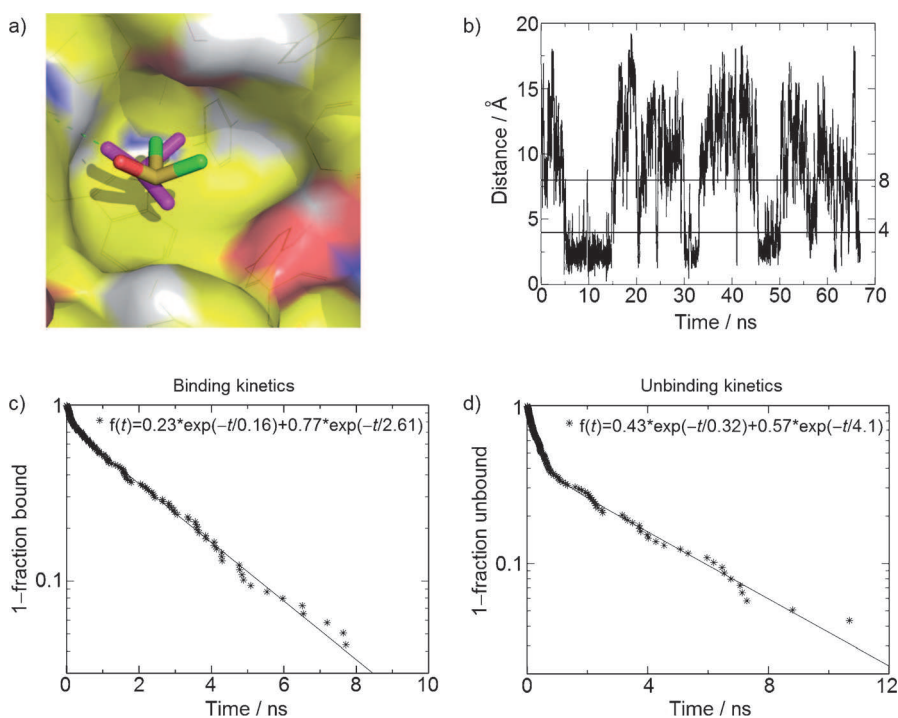


**Figure 2.** Main binding site and (un)binding kinetics. Top: a) The most populated DMSO binding mode observed in the MD simulations (carbon atoms in green) is essentially identical to the binding mode in the X-ray structure (magenta; PDB: 1D7H<sup>[13]</sup>). The surface of FKBP is colored according to atom type: carbon (yellow), nitrogen (blue), oxygen (red). White patches correspond to hydrogen atoms bound to nitrogen and oxygen atoms. b) Time series of distance between FKBP active site center and closest DMSO molecule from one of the ten MD simulations. Bottom: Cumulative distribution  $f(t)$  of the c) binding time and d) unbinding time:  $f(t) = \int_0^t p(\tau) d\tau$ , where  $p$  is the probability distribution of the binding and unbinding time, respectively. Binding and unbinding events are defined by a separation between the centers of mass of the FKBP active site and DMSO smaller than 4 Å (binding) and larger than 8 Å (unbinding). These threshold values were chosen upon visual analysis of the time series, and they are shown by horizontal lines in panel b. The same two-phase behavior and similar characteristic times are obtained with slightly different thresholds, e.g., 5 Å for binding and 9 Å for unbinding. The stars represent the binding and unbinding events (137 in each direction) observed in the ten MD runs. The solid lines are double-exponential fits.

cumulative distribution of times of unbinding from the FKBP active site shows a double-exponential behavior with characteristic times of about 4 ns and 0.3 ns for the slow and fast phases, respectively, and both have amplitudes of about 50% (Figure 2d). Geometric clustering (Supporting Information) and visual analysis of the trajectories suggest that the slow phase of unbinding is due solely to events that start from specific binding in the active site, i.e., from the binding mode with the hydrogen bond between the sulfinyl oxygen and the amide NH of Ile56 (Figures 2 and 3). In contrast, the fast phase originates mainly from dissociation events that start from the DMSO molecule involved in nonpolar interactions between the DMSO methyl groups and the aromatic and aliphatic side chains in the FKBP active site, but without the aforementioned intermolecular hydrogen bond. This result explains why only the slow phase was detected in a previous MD study in which all MD runs started from the X-ray structure of the DMSO–FKBP complex.<sup>[11]</sup> The cumulative distribution of times of binding to the active site shows also a double-exponential character with characteristic times of about 2.6 ns and 0.2 ns for the slow and fast phases, respectively (Figure 2c). The slow phase has an amplitude of about 3/4, while the fast phase originates

from unbinding events during which the distance between the centers of mass of DMSO and the FKBP active site atoms transiently exceeds the threshold but DMSO stays in van der Waals contact with the FKBP surface.

Dissociation from the minor site close to Phe15 shows a single-exponential behavior with unbinding time of about 0.4 ns (Supporting Information). The simple time dependence is consistent with the lack of a specific intermolecular hydrogen bond, i.e., the association of DMSO to the Phe15 side chain is due solely to nonspecific hydrophobic contacts. Moreover, the fast characteristic time of dissociation from Phe15 is similar to the one observed for the fast phase of unbinding from the active site as the same type of unspecific interactions are involved.

The multiple events of reversible (un)binding can be used to extract the affinity of DMSO for the main binding site. The dissociation constant derived from the fraction of MD snapshots in which a DMSO molecule is close to either of the

carbon atoms of Val55 ranges from about 150 mM to 500 mM depending on the choice of the distance threshold from 8 to 5 Å, respectively. Using the DMSO distance from the center of the active site (as in Figure 2), a dissociation constant of about 350 mM is obtained (Supporting Information, table S1).

The (un)binding kinetics extracted from the MD simulations can be employed to determine the dissociation constant as the quotient of on- and off-rates. A value of about 250 mM to 350 mM, depending on the binding and unbinding distance thresholds (Supporting Information, table S1), is derived from the reciprocal of the characteristic time of the slow phase obtained from the aforementioned fits of the cumulative distribution of binding and unbinding times, respectively. These two ranges of values are consistent, which indicates that thermodynamic and kinetic analyses yield similar dissociation constants. Importantly, the values extracted from the MD simulations are in agreement with the dissociation constant of 275 mM obtained by NMR chemical-shift change of one of the methyl groups of Val55 upon DMSO titration.<sup>[12]</sup>

In conclusion, we have shown that explicit solvent MD simulations can be used for determining the main site(s), affinities, and kinetics (i.e., on- and off-rates) of DMSO binding to FKBP.

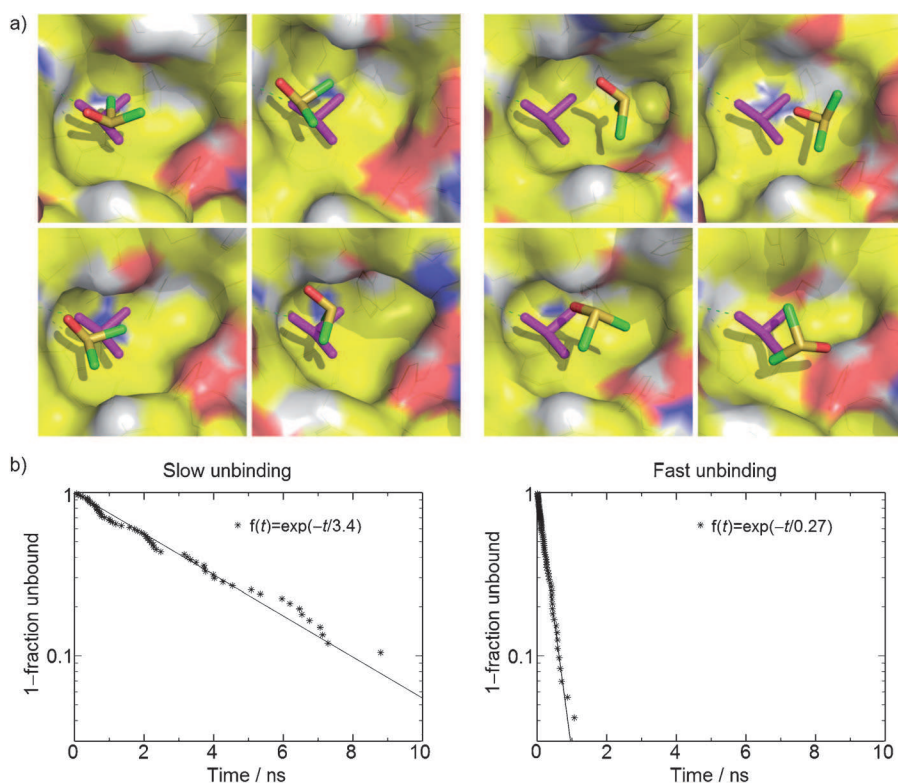


**Figure 3.** Slow and fast unbinding from the FKBP active site. a) Representatives of the four most populated clusters (DMSO carbon atoms in green) and the binding mode in the X-ray structure (DMSO in magenta). The unbinding events from the FKBP active site are divided into two groups depending on the presence (left panels) or absence (right panels) of a hydrogen bond with the amide NH of Ile56 in the preceding binding event. b) Cumulative distribution of unbinding time. The two plots show the unbinding events along the MD simulations (stars) and single-exponential fits (solid lines) for events started from the presence (left) or absence (right) of a hydrogen bond with the NH of Ile56. See also the legend of Figure 2 for details of cumulative distribution.

Despite its small size and number of atoms (only four nonhydrogen atoms), DMSO is appropriate for mapping the physicochemical characteristics of the surface of a protein because its sulfinyl oxygen is a good hydrogen-bond acceptor and its two methyl groups can form hydrophobic contacts. In other words, DMSO is one of the smallest molecules with amphipathic character, and it can be used to design larger inhibitors by pharmacophore search.<sup>[12]</sup> The MD simulations show that the main binding mode of DMSO is in the active site of FKBP where the amide NH of Ile56 acts as hydrogen-bond donor to the sulfinyl oxygen, in agreement with the X-ray structure and NMR spectroscopy data. The constant of dissociation from the FKBP active site was extracted from the multiple binding/unbinding events and found to be in agreement with NMR data. The kinetics of DMSO unbinding from the FKBP active site show a two-phase behavior with a slow and fast phases due to rupture of the hydrogen bond with Ile56 NH and loss of van der Waals contacts with aromatic side chains, respectively. Given their cost and time efficiency, it is likely that in the near future, MD simulations will complement—or even supplement—the state-of-the-art techniques used for fragment-based drug

design like structure–activity relationship investigation by NMR and X-ray crystallography.

### Acknowledgements.

The authors thank Dr. Andreas Vitalis (University of Zürich, Switzerland) for interesting discussions and comments on the manuscript, and Armin Widmer (Novartis Pharma AG, Basel, Switzerland) for the program WITNOTP, which was used for visual analysis of the trajectories. The majority of the calculations were carried out on the Schrödinger computer cluster of the University of Zürich (Switzerland).

**Keywords:** binding kinetics · computational chemistry · fragment-based drug design · FKBP · molecular dynamics

- [1] H. Shuker, P. Hajduk, R. Meadows, S. W. Fesik, *Science* **1996**, *274*, 1531–1534.
- [2] G. Siegal, E. Ab, J. Schultz, *Drug Discovery Today* **2007**, *12*, 1032–1039.
- [3] D. Huang, A. Caffisch, *J. Mol. Recognit.* **2010**, *23*, 183–193.
- [4] O. Guvench, A. D. MacKerell, Jr., *PLoS Comput. Biol.* **2009**, *5*, e1000435.
- [5] J. Seco, F. Luque, X. Barril, *J. Med. Chem.* **2009**, *52*, 2363–2371.
- [6] R. Curcio, A. Caffisch, E. Paci, *Protein Sci.* **2005**, *14*, 2499–2514.
- [7] F. Ytreberg, *J. Chem. Phys.* **2009**, *130*, 164906.
- [8] F. Colizzi, R. Perozzo, L. Scapozza, M. Recanatini, A. Cavalli, *J. Am. Chem. Soc.* **2010**, *132*, 7361–7371.
- [9] S. Burendahl, C. Danculescu, L. Nilsson, *Proteins Struct. Funct. Bioinf.* **2009**, *77*, 842–856.
- [10] N. Basse, J. L. Kaar, G. Settanni, A. C. Joerger, T. J. Rutherford, A. R. Fersht, *Chem. Biol.* **2010**, *17*, 46–56.
- [11] D. Huang, A. Caffisch, *PLoS Comput. Biol.* **2011**, *7*, e1002002.
- [12] C. Dalvit, P. Floersheim, M. Zurini, A. Widmer, *J. Biomol. NMR* **1999**, *14*, 23–32.
- [13] B. R. Brooks, C. L. Brooks III, A. D. Mackerell, Jr., L. Nilsson, R. J. Petrella, B. Roux, Y. Won, G. Archontis, C. Bartels, S. Boresch, A. Caffisch, L. Caves, Q. Cui, A. R. Dinner, M. Feig, S. Fischer, J. Gao, M. Hodoscek, W. Im, K. Kuczera, T. Lazaridis, J. Ma, V. Ovchinnikov, E. Paci, R. W. Pastor, C. B. Post, J. Z. Pu, M. Schaefer, B. Tidor, R. M. Venable, H. L. Woodcock, X. Wu, W. Yang, D. M. York, M. Karplus, *J. Comput. Chem.* **2009**, *30*, 1545–1614.
- [14] M. Seeber, M. Cecchini, F. Rao, G. Settanni, A. Caffisch, *Bioinformatics* **2007**, *23*, 2625–2627.
- [15] P. Burkhard, P. Taylor, M. D. Walkinshaw, *J. Mol. Biol.* **2000**, *295*, 953–962.

Received: May 12, 2011

Published online on June 14, 2011